

A Sensorless, Inherently Compliant Anthropomorphic Musculoskeletal Hand Driven by Electrohydraulic Actuators

Misato Sonoda^{1,2}, Ronan Hinchet¹, Amirhossein Kazemipour¹, Yasunori Toshimitsu¹, and Robert K. Katzschmann¹

Abstract—Robotic manipulation in unstructured environments requires end-effectors that combine high kinematic dexterity with physical compliance. While traditional rigid hands rely on complex external sensors for safe interaction, electrohydraulic actuators offer a promising alternative. This paper presents the design, control, and evaluation of a novel musculoskeletal robotic hand architecture powered entirely by remote Peano-HASEL actuators, specifically optimized for safe manipulation. By relocating the actuators to the forearm, we functionally isolate the grasping interface from electrical hazards while maintaining a slim, human-like profile. To address the inherently limited linear contraction of these soft actuators, we integrate a 1:2 pulley routing mechanism that mechanically amplifies tendon displacement. The resulting system prioritizes compliant interaction over high payload capacity, leveraging the intrinsic force-limiting characteristics of the actuators to provide a high level of inherent safety. Furthermore, this physical safety is augmented by the self-sensing nature of the HASEL actuators. By simply monitoring the operating current, we achieve real-time grasp detection and closed-loop contact-aware control without relying on external force transducers or encoders. Experimental results validate the system’s dexterity and inherent safety, demonstrating the successful execution of various grasp taxonomies and the non-destructive grasping of highly fragile objects, such as a paper balloon. These findings highlight a significant step toward simplified, inherently compliant soft robotic manipulation.

I. INTRODUCTION

Robotic manipulation in unstructured environments demands end-effectors that possess both high kinematic dexterity and physical compliance. Traditional rigid robotic hands, typically driven by electromagnetic motors, excel in precision and payload capacity. However, they lack inherent physical compliance, necessitating complex and expensive external sensors [1], [2], [3], such as multi-axis force/torque sensors or tactile arrays, to ensure safe interactions with fragile objects, unknown shapes, or humans. This reliance on sensors significantly increases the system’s complexity, weight, and computational overhead.

Soft robotics has emerged as a compelling alternative, utilizing compliant materials and structures to naturally adapt to object geometries and absorb external impacts. While fluid-driven soft actuators offer excellent compliance [4], [5], they typically require bulky compressors, valves, and

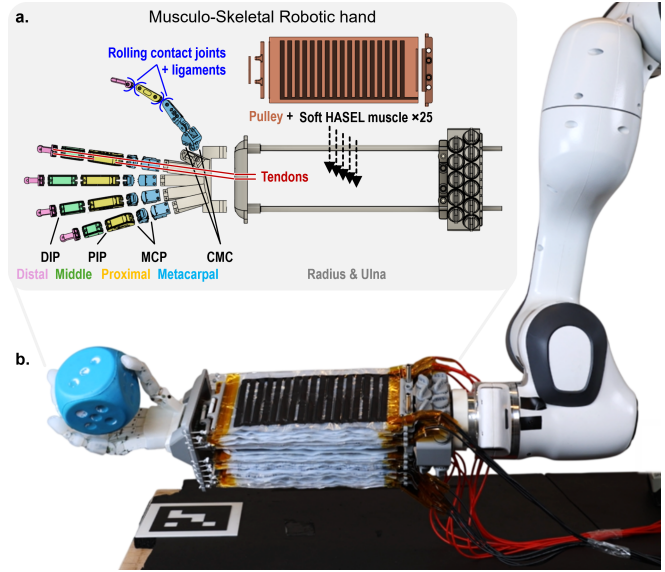


Fig. 1. A tendon-driven robotic hand system actuated with HASEL actuators. (a) Soft HASEL muscle actuators in the forearm drive the fingers via tendon transmission and pulley mechanisms, enabling compliant finger motion through rolling-contact joints. (b) The proposed hand system is grasping a cube. All fingers can be controlled independently.

tubes. Recently, electrohydraulic actuators, specifically Hydraulically Amplified Self-Healing Electrostatic (HASEL) actuators, have gained attention [6], [7]. They combine the fast response times of dielectric elastomer actuators with the versatility of fluidic systems, offering muscle-like actuation that is inherently compliant and capable of self-sensing, as reported in many robotic applications [8], [9].

Despite these advantages, the integration of HASEL actuators into highly dexterous robotic hands remains a challenge. Most existing HASEL-based grippers [6], [10], rely on the direct bending or deformation of the actuators themselves. While suitable for simple pinching or wrapping motions, this direct-actuation approach severely limits the grasp taxonomy and kinematic precision compared to anthropomorphic skeletal designs driven through tendons. Furthermore, the contraction strain of HASEL actuators is typically limited to below 15 % [11], which is often insufficient to fully drive the large joint excursions of human-inspired hand and forearm designs. Additionally, placing high-voltage actuators directly at the grasping interface raises safety concerns and increases the bulkiness of the fingers.

Recent advancements have demonstrated the potential

¹Soft Robotics Lab, ETH Zurich, Switzerland

²The University of Tokyo, Japan

{msonoda, rhinchet, akazemi, ytoshimitsu, rkk}@ethz.ch

of HASEL-driven prosthetics to overcome some of these kinematic limits. Most notably, the high-speed prosthetic finger presented in [9] achieved impressive fingertip forces (> 1 N) and a large range of motion (77°). This was accomplished by coupling seven HASEL actuators in parallel to pull the base of a rigid four-bar linkage mechanism. However, this rigid linkage and parallel actuation strategy was dedicated to a single digit. Directly replicating this approach for all fingers of an anthropomorphic hand would result in bulk, complex routing, and a loss of the inherent physical compliance desired in soft robotics. Scaling these concepts to a fully integrated, multi-fingered hand requires a shift from maximizing the raw power of an isolated digit to optimizing system-level integration, space efficiency, and interactive safety.

To address these challenges and significantly extend the HASEL-driven prosthetics approach, this paper presents a novel, integrated musculoskeletal robotic hand architecture powered entirely by remote Peano-HASEL actuators. Our approach bridges the gap between soft actuator compliance and rigid kinematic dexterity by synergizing a remote actuation paradigm with a compliant, human-inspired transmission. Building upon a tendon-driven architecture, we relocate the HASEL actuators to a human-sized forearm, isolating the grasping interface from electrical hazards and maintaining a slim, human-like hand profile. To overcome the inherent stroke limitations of the soft actuators without relying on massive parallel stacks, we implement a 1:2 pulley routing mechanism that mechanically amplifies the tendon displacement, intending to enable the full range of motion across the rolling-contact finger joints. Crucially, our design focuses on optimizing the system for the safe manipulation of fragile objects. Rather than pursuing high payload capacity, the resulting architecture prioritizes compliant interaction by leveraging the intrinsic force-limiting characteristics of HASEL actuators. This ensures non-destructive contact with delicate items and environments, providing a high level of inherent safety without the need for complex, high-bandwidth active force control.

The main contributions of this paper are threefold:

- The holistic design of an anthropomorphic robotic hand optimized for safe manipulation. By synergizing a remote-actuation paradigm with a stroke-amplifying transmission, this architecture simultaneously achieves a slim, human-like form factor, electrical isolation for enhanced safety, and the kinematic range necessary for dexterous manipulation.
- The implementation of a sensorless manipulation approach that leverages the capacitive nature of HASEL actuators via operating current monitoring. This enables real-time grasp detection and safe, closed-loop control for delicate grasping without the need for external encoders or force sensors.
- An experimental validation of the system’s dexterity and inherent safety. We demonstrate the successful execution of various grasp postures derived from standard taxonomies, as well as the non-destructive manipulation of

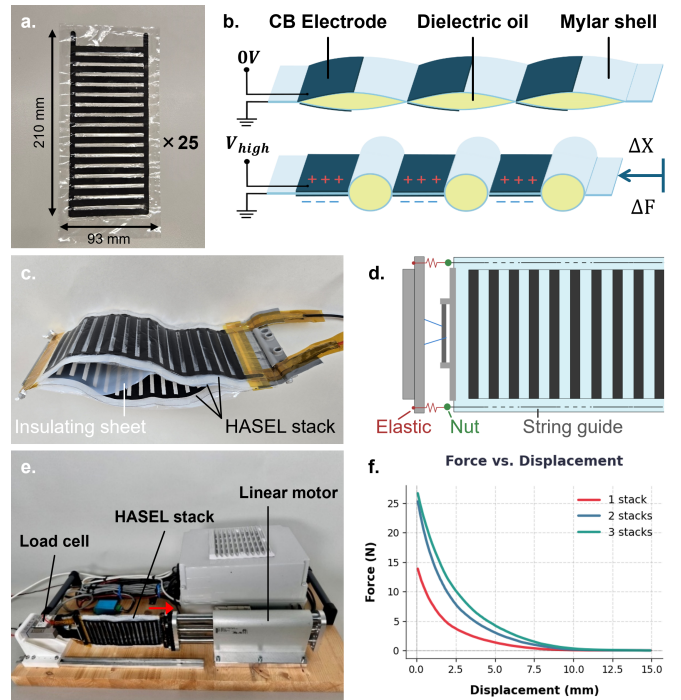


Fig. 2. **Soft Muscle Stacking.** (a) A fabricated Peano-HASEL actuator is 210 mm by 93 mm. (b) Actuation principle of the Peano-HASEL actuator proposed in [7]. (c) Connected actuator stack forming a soft muscle. (d) Guiding structure of the actuators. (e) Force-displacement characterization setup using a linear motor and a load cell. (f) The force-displacement characteristics of single, double, and triple stacked Peano-HASEL configurations.

extremely fragile objects, such as an origami paper balloon, highlighting the practical utility of a limited-force, high-compliance design in sensitive environments.

II. SYSTEM DESIGN

A. Actuator Design and Characterization

Peano-HASEL actuators [7] were fabricated using the following methods: the basic structure consists of a flexible pouch made from $25 \mu\text{m}$ Mylar (PET) films. Carbon ink electrodes were screen-printed onto the films and cured. The pouches were then filled with a liquid dielectric (silicone oil, 5 cSt) and heat-sealed.

To amplify the output force for the robotic hand, multiple Peano-HASEL actuators Fig. 2(a) were connected in parallel to form strong actuator stacks. To ensure safe operation at high voltages and prevent electrical arcing or short circuits, silicone spray was applied to the outer surfaces of the actuators. Furthermore, $50 \mu\text{m}$ PTFE sheets were interleaved between each actuator in the stack; these serve the dual purpose of providing electrical insulation and minimizing inter-actuator friction during contraction.

To determine the optimal number of parallel actuators for each finger joint, the force-displacement characteristics of the stacks were experimentally evaluated. The actuators were secured in a custom pull tester equipped with a linear motor (C1250-MI-XC-0S-000, LinMot) and a load cell (Model 614, Tedeia Huntleigh). While applying an operating voltage of 5.5

kV, the linear motor stretched the actuators by 15 mm at a constant velocity of 0.5 mm/s, continuously recording the contraction force. The resulting force-displacement curves for single (10 g), double (22 g), and triple stack (34 g) configurations are compared in Fig. 2(f). While increasing the number of parallel units enhances the output force, it simultaneously adds weight and bulk to the forearm. Therefore, the stack configuration for each joint was determined by balancing the kinematic and task requirements of the finger against the overall weight and space constraints of the system.

In the hand design, the distal and proximal interphalangeal (DIP/PIP) joints require a maximum tendon excursion of approximately 12 mm to reach a 90° flexion. To accommodate the limited stroke length of the HASEL actuators, our design incorporates a 1:2 pulley routing system on top of the actuator packs. This mechanism halves the required displacement, meaning the 12 mm tendon excursion corresponds to only a 6 mm linear contraction of the actuator. For these joints, the 2-stack configuration provided sufficient contraction force across this 6 mm operating range (ranging from 25.3 N at the initial position to 2.0 N at a 6 mm contraction) while keeping the system lightweight.

Conversely, the metacarpophalangeal (MCP) joints require a larger tendon excursion of up to 17 mm—which translates to an 8.5 mm actuator contraction through the pulley system—and typically bear higher mechanical loads during power grasping. Consequently, the heavier 3-stack configuration was selected specifically for the MCP joints to ensure an adequate stroke margin and sufficient gripping capability.

B. Robotic Hand Design

The mechanical design of the proposed robotic hand is based on a circular rolling contact joint design [12], [13]. These joints allow the center of rotation to shift dynamically during bending, enabling smooth, space-efficient flexion.

The index, middle, ring, and pinky fingers are composed of three rigid phalanges (proximal, intermediate, and distal) connected by rolling contact joints with ligaments at the metacarpophalangeal (MCP), proximal interphalangeal (PIP), and distal interphalangeal (DIP) joints. It allows for 90° joint flexion and 30° abduction. The tendon-routing includes independent flexor and extensor tendons to drive the MCP joint, while the PIP and DIP joints are mechanically coupled to flex and extend synergistically, similar to a human hand.

To enable human-like opposition grasps, the thumb features a distinct kinematic structure incorporating an interphalangeal (IP) and an MCP rolling contact joint, while using a pin joint based carpometacarpal (CMC) joint. In this research, the abduction of the CMC joint was mechanically fixed, resulting in a total of two active degrees of freedom (DOF) for the thumb.

The rigid palm serves as the structural support of the fingers and smoothly routes the tendons toward the forearm. To enhance grasping performance and safety, the palm and

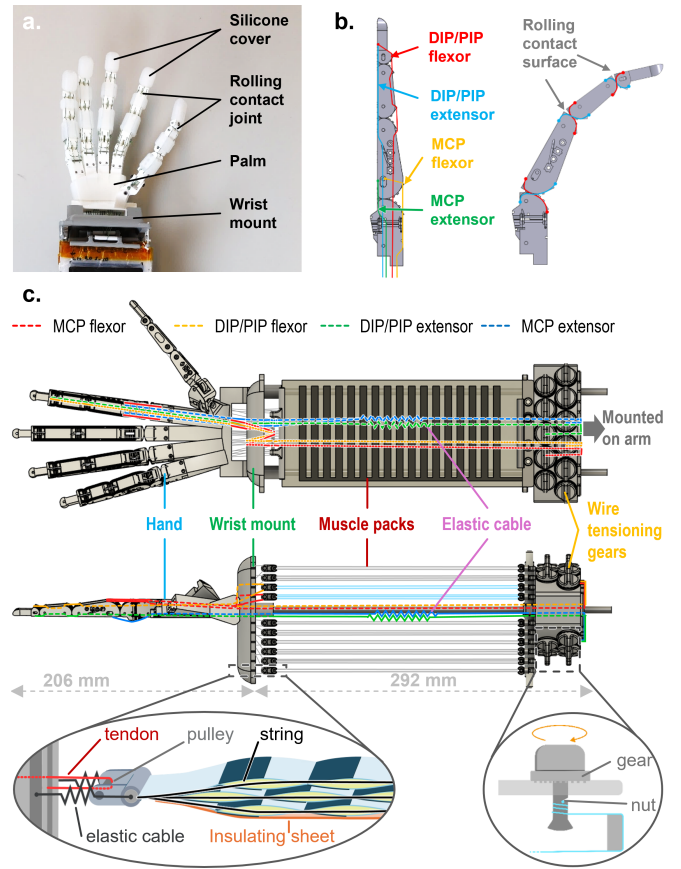


Fig. 3. **Tendon-Driven Hand Design.** (a) Overview of the modular robotic hand. (b) Flexor and extensor tendon routing of the index finger, demonstrating the rolling contact joints and coupled PIP/DIP mechanism. (c) Actuator packs are stacked in parallel in the forearm (e.g., 2-stack for DIP/PIP, 3-stack for MCP). The flexor tendons utilize a pulley system attached to the actuators, while the extensor tendons are connected in series with elastic cords for passive restoration. All tendons are anchored and adjusted at the wire tensioning gears located at the bottom.

finger surfaces are enclosed in a custom-molded soft silicone skin (Dragon Skin 10, Smooth-On). This compliant skin improves the grasp and helps prevent object slippage.

C. Transmission Mechanism

To convert the linear contraction of the HASEL actuators into independent finger movements, the robotic hand employs a flexor–extensor tendon routing architecture, as illustrated in Fig. 3(c), with active flexion and passive elastic extension.

Flexor Tendon Routing: The finger’s flexion is actively driven by the HASEL actuator stacks located in the forearm. To achieve the 1:2 stroke amplification discussed in Section II-A, the flexor tendons are routed through a pulley attached to the top of the actuator stacks. Specifically, the tendon enters the forearm through the wrist mount, wraps around a pulley attached to the top (distal end) of the actuator stack, and loops back to a secondary routing point on the wrist mount. From there, the tendon travels down through the central free space of the forearm—between the actuator stacks—and is anchored to the wire tensioning gears at

the base. This configuration effectively doubles the tendon excursion relative to the actuator’s linear contraction while maintaining the system’s compact form factor.

Extensor Tendon Routing: Conversely, finger extension is achieved passively through an elastic return mechanism. The extensor tendons pass through a central hole in the wrist mount and are connected in series with elastic cords within the forearm. The proximal ends of these elastic cords are connected to tendons that anchor to the bottom tensioning gears.

Furthermore, to maintain structural stability during dynamic movements, each actuator stack is laterally reinforced. Specifically, the sides of the actuators are sewn with fishing lines, which are tensioned by serially connected elastic cables. As illustrated in Fig. 2(d), this arrangement keeps the actuators properly aligned and prevents buckling during contraction. Finally, all flexor and extensor tendons can be individually calibrated via the tensioning gears located at the base of the forearm, allowing for precise adjustment of the hand’s resting tension and joint alignment.

D. Experimental Setup

The fully assembled robotic hand was mounted on Franka Research 3 (Franka Robotics GmbH) to conduct dynamic interaction and grasping experiments. All experiments and real-time control loops were executed using a data acquisition (DAQ) system (myDAQ, National Instruments) interfaced with MATLAB custom scripts. The control signals generated by the DAQ were subsequently amplified by a high-voltage amplifier (Trek 610 C, Trek, Inc.), providing driving voltages of up to 5.5 kV (and up to 6.0 kV specifically for contact-aware control tasks) to the HASEL actuator stacks.

To enable the current-sensing, contact-aware grasp control and grasp detection discussed in Section III-D, the applied voltage and operating current were continuously measured. This was achieved using the built-in monitor channels of the high-voltage amplifier, which fed analog signals directly back to the DAQ system.

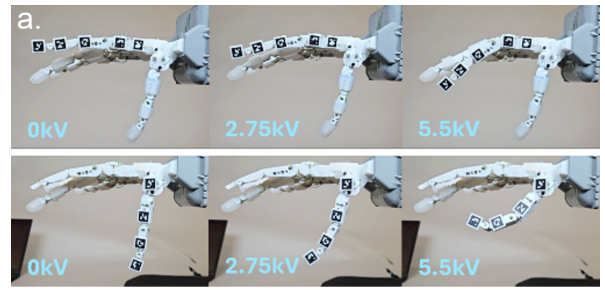
III. EXPERIMENTAL RESULTS

A. Characterization of Finger Performance

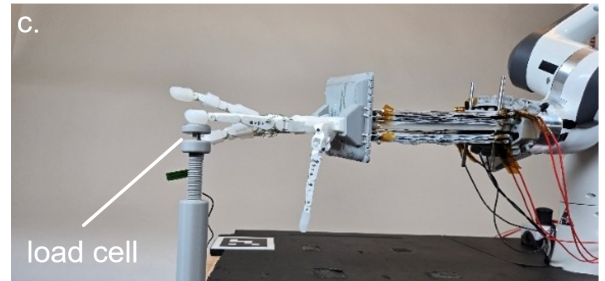
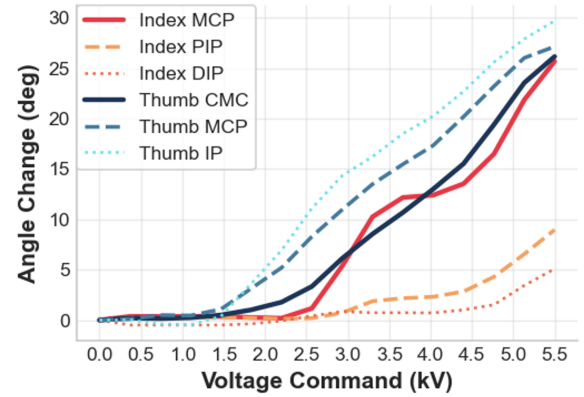
In this section, we evaluate the fundamental characteristics of the proposed tendon-driven robotic hand, specifically focusing on the kinematic motion range and the static fingertip force of the index finger and thumb under varying input voltages.

1) Evaluation of Finger Motion Range: To evaluate the operating range of the thumb and index finger, we investigated the relationship between the applied voltage to the actuators and the corresponding variations in joint angles. AprilTags were attached to each joint to serve as position and posture references. We recorded the finger motions using a fixed camera at 30 fps while applying a 1 s voltage ramp signal to the actuators.

The relationship between the applied voltage and the joint angles is shown in Fig. 4(b), with the corresponding finger postures illustrated in Fig. 4(a). As expected, the



b. Voltage vs. Joint Angles



d. Voltage vs. Fingertip force

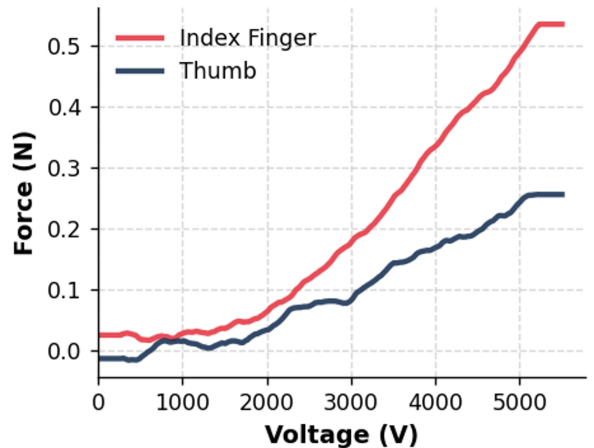


Fig. 4. **Characterization of the index finger and thumb performance.** (a, b) A 1 s ramp signal was applied to the index finger and thumb, and the motion range of each joint was measured. (c, d) Under the same input conditions, the fingertip force was measured.

joint angles of both fingers increase as the applied voltage increases. Based on the actuator force-displacement charac-

terization and the 1:2 pulley mechanism, the fingers should theoretically achieve a full range of motion. However, the experimental results reveal two distinct limitations in the practical actuation.

First, a deadband is observed in the low-voltage region. This is primarily attributed to the initial static friction in the tendon-routing system and mechanical backlash at the joints, which require a minimum driving force from the actuator to initiate flexion.

Second, the maximum joint angle achieved in practice is limited to approximately 30° , falling significantly short of the intended 90° flexion. Although mechanical amplification is present, the effective driving force is restricted during operation. This limitation primarily arises from the friction within the tendon-routing system and the increased friction between the actuator packs as they contract. Consequently, the current actuators reach their force limits under the system's dynamic load before achieving their full motion.

2) *Evaluation of Fingertip Force:* Next, we evaluated the static fingertip force exerted by the thumb and index fingers. The experimental setup is shown in Fig. 4(c). A load cell (DYLY-109, Daysensor) was fixed on a vertical pole, with a button on top. Both the thumb and index finger were initially set to their fully extended (straight) postures and positioned to press directly on the load cell. During the measurement, the applied voltage to the actuators was gradually increased, and the corresponding exertion force on the load cell was recorded.

The resulting voltage-force relationship for both fingers is plotted in Fig. 4(d). At the maximum applied voltage of 5.5 kV, the index and thumb fingers generated maximum fingertip forces of 0.53 N and 0.26 N, respectively. The difference in the maximum generated force between the two digits is likely due to differences in their specific tendon-routing paths, friction losses, and mechanical advantages.

To contextualize these performance metrics, it is important to compare them with existing HASEL-driven systems. For instance, the high-speed prosthetic finger presented in [9] demonstrated a larger range of motion (77°) and forces exceeding 1 N. However, those results were achieved by utilizing parallel HASEL actuator stacks to drive a rigid four-bar linkage for a single digit—an approach that maximizes raw power and transmission efficiency at the cost of dedicated volume and physical compliance. In contrast, the restricted articulation and lower absolute force observed in our system represent a deliberate trade-off to accommodate a multi-fingered architecture within a space-constrained, human-sized forearm. By employing a compliant tendon-driven transmission and rolling-contact joints, our design prioritizes holistic integration and gentle adaptability over the maximized kinematics of an isolated, rigid joint. Despite the relatively low force values, they align with our objective of inherent safety and prove sufficient for the stable, non-destructive grasping of lightweight, fragile objects.

B. Compliance and Backdrivability

Compliance is a critical characteristic of robotic hands for safely interacting with humans and unstructured environments, allowing them to passively deform and mitigate excessive forces during unexpected impacts. The proposed tendon-driven hand derives its inherent compliance from both the tendon-routing mechanism and the soft structure of the HASEL actuators. Because the actuators consist of flexible dielectric pouches filled with liquid, external forces can easily redistribute the internal fluid, resulting in low mechanical impedance.

In the unpowered state, the entire system exhibits high flexibility. As shown in Fig. 5(a, b), the actuator packs located in the forearm can passively deform and accommodate twisting motions when manipulated by a human hand.

To evaluate the system's adaptability under active conditions, we conducted an object removal test. A constant 5.5 kV voltage was applied to the actuators to maintain a grasp on an object. When a human manually pulled the grasped object, the fingers passively extended, allowing the object to be removed smoothly without damaging the mechanism or the object itself (Fig. 5(c)).

Furthermore, we evaluated the dynamic backdrive behavior during sudden collisions. A tennis ball was thrown at the fingers while they were actively flexed under a constant applied voltage. As demonstrated in Fig. 5(d), the proposed hand absorbed the impact by significantly deforming backward and subsequently returning to its initial flexed posture. In contrast, a conventional motor-driven hand subjected to the same impact exhibited a rigid response with minimal deformation under the impact (Fig. 5(e)).

These results show that the proposed HASEL-driven robotic hand system possesses inherently high compliance and backdrivability. This robust and passive adaptability makes the system highly suitable for safe physical human-robot interaction in collaborative and service robotics applications.

C. Versatile Grasping

To evaluate the practical grasping performance and versatility of the proposed tendon-driven hand, we conducted empirical demonstrations across diverse grasp taxonomies. Based on standard human grasp models [14], [15], we tested the hand's ability to execute three representative grasping postures: 1) pinching (thumb and index finger), 2) tripod grasp (thumb, index, and middle fingers), and 3) power grasp (all fingers). For each grasping task, a 1 s ramp voltage signal was applied to reach the target actuation level, followed by a constant holding voltage of 5.5 kV.

As shown in Fig. 6, the hand successfully adapted to various levels of object geometry without requiring complex control schemes. Specifically, the hand achieved stable pinching of an 18 g mushroom and a 49 g cube (Fig. 6(a, b)), a tripod grasp on a 107 g soft stuffed toy (Fig. 6(c)), and a power grasp enveloping a 26 g empty PET bottle (Fig. 6(d)). In all configurations, the fingers naturally conformed to the

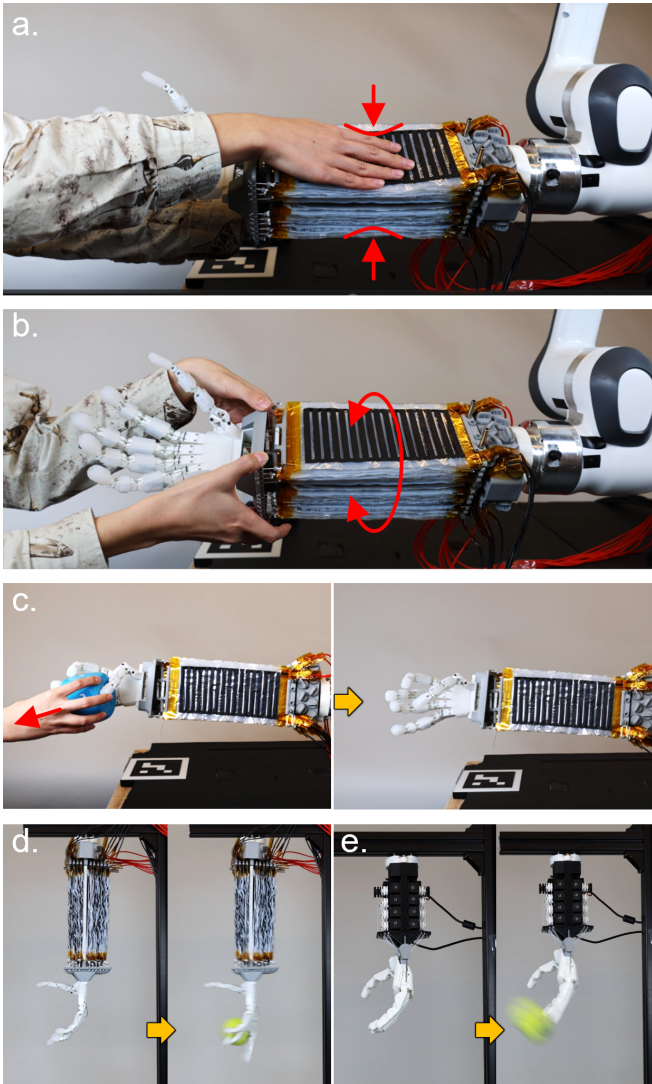


Fig. 5. **The proposed musculoskeletal hand system is inherently compliant.** (a, b) Demonstration of the mechanical compliance of the actuator packs in the forearm. The actuator packs deform when pushed by a human hand and accommodate twisting of the forearm. (c) The grasped object can be easily removed from the hand while constant voltage is applied, demonstrating its backdrivability. (d, e) Comparison of collision responses while actuators are active: the proposed HASEL-driven hand safely absorbs the impact of a tennis ball through large deformation, whereas a conventional motor-driven hand exhibits a rigid response.

objects’ surfaces, maintaining stable grasps without noticeable slip or posture deviation.

These results confirm that the combination of multiple contact points and soft actuation enables stable grasping of light objects, proving the system’s adaptability for a wide range of manipulation tasks.

D. Current Sensing Feedback Control

Conventional robotic hands often rely on dedicated external sensors, such as encoders and force sensors, to measure bending velocity and contact states. However, these sensors increase system complexity, wiring, and overall weight, which restricts the scalable design of multi-fingered hands. To reduce this reliance on external sensing hardware, we

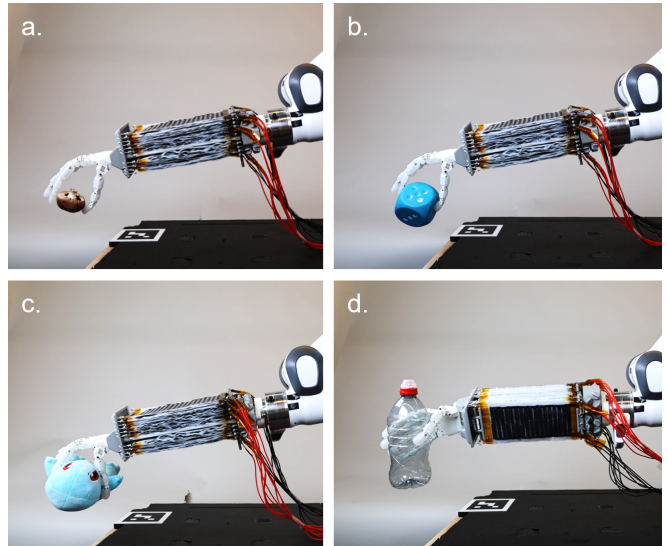


Fig. 6. **Demonstration of versatile grasp taxonomies adapting to different object properties.** (a, b) Pinching an 18 g mushroom and a 49 g cube using the thumb and index finger. (c) Tripod grasp of a 107 g soft stuffed toy. (d) Power grasp enveloping a 26 g empty PET bottle.

implemented a self-sensing feedback method that leverages the inherent physical properties of HASEL actuators. Since a HASEL actuator consists of a dielectric fluid and electrodes, it essentially functions as a variable capacitor. While previous studies have achieved state estimation by observing variations in capacitance [8], [10], such estimations are typically derived from measured voltage and current through secondary computations. In contrast, our study leverages the operating current as a direct, physical source of information regarding the actuator’s motion state. Because the current flow is fundamentally governed by the rate of geometric deformation, it serves as a robust indicator of the actuator’s real-time kinematic activity. By bypassing the secondary computation required for capacitance estimation, our method minimizes computational overhead and avoids the potential for noise amplification. We demonstrate that simply monitoring this single physical quantity allows the system to reliably achieve behaviors such as grasp detection and contact-aware control, without the need for any supplementary sensors or the estimation of additional physical variables.

A first-order model for the actuator’s displacement current is

$$\dot{i}(t) = C(t) \frac{dv(t)}{dt} + v(t) \frac{dC(t)}{dt}, \quad (1)$$

where $C(t)$ is the capacitance, $v(t)$ is the applied voltage, and t is time. The second term, $v(t) \frac{dC(t)}{dt}$, is the dynamic component that depends on the rate of geometric deformation. When the actuator’s motion is physically constrained (e.g., upon contacting an object), the rate of capacitance change drops, resulting in a noticeable decrease in the drawn current. By monitoring this current in real-time, we can estimate the actuator’s motion state and detect external contacts without additional sensors. In this study, we specifically monitored the operating current of the actuator

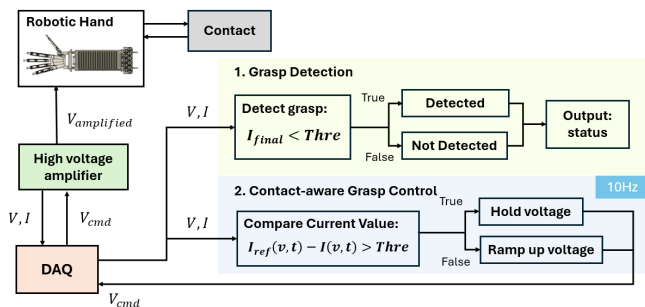


Fig. 7. **Overview of the current sensing feedback control mechanism.** The algorithms utilize real-time current measurement for Grasp Detection and Contact-Aware Grasp Control.

stack corresponding to the index MCP joint, as it exhibited the most distinct and reliable current variations upon contact with various objects. The voltage and current signals are continuously monitored directly from the high-voltage amplifier at a sampling rate of 1 kHz.

1) *Grasp Detection*: We developed a grasp detection algorithm based on monitoring the actuator’s operating current. During the grasping motion, a ramp voltage is applied to the actuator. The algorithm evaluates the real-time current against a predefined threshold. This threshold was determined by pre-measuring the current profiles of both free-motion and successful grasping scenarios; we then selected an optimal value that provides a stable and repeatable distinction between the two states.

When the hand grasps a rigid object (e.g., a cube), the resulting physical constraint halts further deformation of the fingers, causing the current to drop below the threshold. Conversely, in a free-motion scenario (no object), the current remains above the threshold due to the continuous geometric deformation. Experimental results (Fig. 8) demonstrated that this threshold-based evaluation successfully detects the presence of a grasped object purely from the electrical state of the actuator.

2) *Contact-Aware Control for Delicate Grasping*: To further demonstrate the utility of the self-sensing approach, we implemented a closed-loop contact-aware control strategy to grasp fragile objects, such as a paper balloon, without crushing them. The control algorithm continuously compares the real-time operating current with a pre-recorded baseline current trajectory (obtained during free motion). When the difference between the measured current and the baseline exceeds a specific threshold—indicating that the fingers have made contact with the object—the controller stops increasing the voltage and holds it at the current level. As shown in Fig. 9, this strategy effectively halts finger flexion upon contact, bounding the applied grasping force and preventing structural damage to the delicate object.

These results demonstrate that safe, contact-aware manipulation and effective force limitation can be achieved by directly monitoring the actuator’s operating current, thereby enhancing the practical applicability of the proposed soft robotic hand without the need for external force sensors.

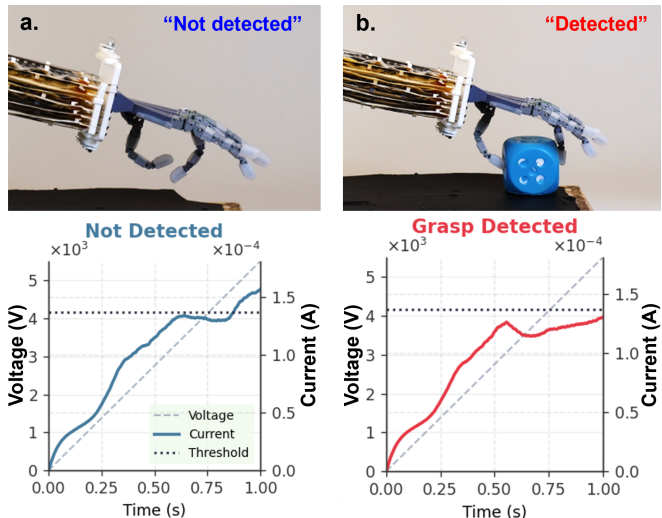


Fig. 8. **Results of the grasp detection experiment.** The current drops significantly when the finger motion is constrained by an object, allowing threshold-based detection.

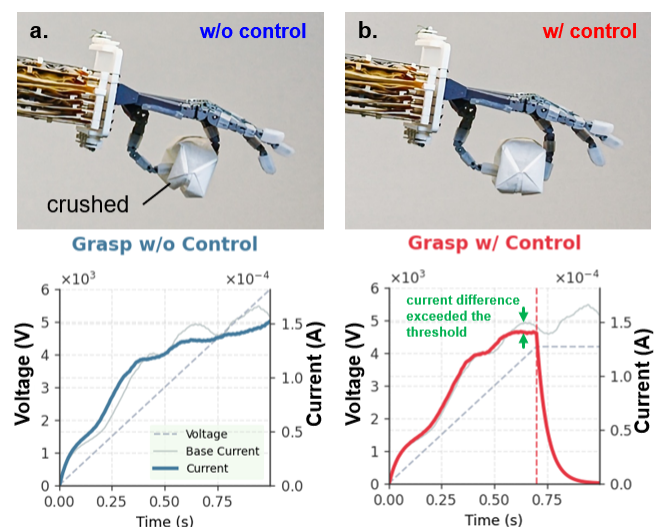


Fig. 9. **Results of the contact-aware grasp control.** By holding the voltage when the current deviates from the free-motion baseline, the hand successfully grasps a fragile paper balloon without crushing it.

IV. DISCUSSION AND CONCLUSION

In this paper, we presented the design, control, and evaluation of an integrated musculoskeletal robotic hand architecture powered entirely by remote Peano-HASEL actuators. By integrating these electrohydraulic artificial muscles with a compliant, human-inspired tendon-driven architecture, we successfully developed a multi-fingered hand that bridges the gap between physical compliance and kinematic dexterity. The implementation of a remote actuation paradigm and a 1:2 pulley-based transmission not only mitigated electrical hazards and stroke limitations but also facilitated a slim, human-like form factor. Experimental results demonstrated the system’s high versatility, showing its ability to execute various grasp taxonomies and gently manipulate objects of diverse sizes and shapes.

Furthermore, this physical safety is augmented by utilizing the self-sensing nature of the HASEL actuators. By monitoring the operating current, we successfully achieved grasp detection and closed-loop contact-aware control without relying on external sensors, such as encoders or force transducers. This self-sensing capability allowed the hand to delicately grasp highly fragile objects, such as a paper balloon, without causing structural damage. These findings highlight the potential of HASEL-driven systems to simultaneously achieve high physical safety and compliance while simplifying both the mechanical design and control architectures in soft robotic end-effectors.

Despite these promising results, the current system presents several limitations that outline a roadmap for future optimization. First, driving the HASEL actuators requires high voltages, which necessitates stringent electrical insulation to ensure practical safety. Second, the fingers' maximum output force and effective range of motion are currently limited. While this force level is inherently suited for the gentle manipulation of fragile objects as demonstrated in this work, it constrains the hand's versatility for tasks requiring higher payloads. As discussed, these kinematic and force limitations represent a deliberate trade-off: we prioritized a multi-fingered, compliant architecture—necessitating the routing of multiple tendons through a space-constrained wrist—over the use of highly efficient but rigid transmissions with larger parallel actuator stacks. The effective force transmitted from the actuators to the fingertips is significantly attenuated due to mechanical backlash within the components, alongside friction in both the tendon-routing pathways and the contracting actuator packs.

Future work will focus on addressing these mechanical limitations to improve the actuation performance. Incorporating low-friction materials and refining the pulley geometry will be essential to minimize energy losses. The low-voltage deadband could be mitigated by adopting an antagonistic muscle configuration; preloading both opposing muscles will minimize mechanical slack and help overcome initial static friction. Furthermore, to bridge the gap between the currently limited range of motion and full finger articulation, we aim to explore the integration of new types of artificial muscles that can deliver higher stroke and force under continuous dynamic loads.

Future work will also involve comprehensive quantitative benchmarking. While this study focuses on system integration, future evaluations will include direct comparisons with existing HASEL-based grippers and other soft robotic hands. We also plan to expand the preliminary comparison with motor-driven systems (Fig. 5(e)) by analyzing rigorous metrics such as grasp stability, bandwidth, and energy efficiency to clearly define the trade-offs of our musculoskeletal architecture.

Finally, while the current approach relies on a simple current-threshold mechanism, we plan to advance the self-sensing capabilities by incorporating a broader range of physical data. By integrating operating current with other physical information, such as capacitive variations, the system will

be able to achieve more information-rich sensing. Observing these capacitive variations will enable the continuous estimation of precise joint kinematics. This progression toward more sophisticated control will facilitate complex, dynamic in-hand manipulation tasks, further pushing the boundaries of sensorless soft robotic hands.

ACKNOWLEDGMENT

This work was supported by the SNSF Project Grant #200021_215489. This support was instrumental in the development of this research.

REFERENCES

- [1] "Developments in dextrous hands for advanced robotic applications," in *Proceedings World Automation Congress, 2004.*, vol. 15, 2004, pp. 123–128.
- [2] H. Liu, K. Wu, P. Meusel, N. Seitz, G. Hirzinger, M. Jin, Y. Liu, S. Fan, T. Lan, and Z. Chen, "Multisensory five-finger dexterous hand: The dlr/hit hand ii," in *2008 IEEE/RSJ international conference on intelligent robots and systems*. IEEE, 2008, pp. 3692–3697.
- [3] A. M. Dollar and R. D. Howe, "The highly adaptive sdm hand: Design and performance evaluation," *The international journal of robotics research*, vol. 29, no. 5, pp. 585–597, 2010.
- [4] R. Deimel and O. Brock, "A novel type of compliant and underactuated robotic hand for dexterous grasping," *The International Journal of Robotics Research*, vol. 35, no. 1-3, pp. 161–185, 2016.
- [5] F. Ilievski, A. D. Mazzeo, R. F. Shepherd, X. Chen, and G. Whitesides, "Soft robotics for chemists," 2011.
- [6] E. Acome, S. K. Mitchell, T. Morrissey, M. Emmett, C. Benjamin, M. King, M. Radakovitz, and C. Keplinger, "Hydraulically amplified self-healing electrostatic actuators with muscle-like performance," *Science*, vol. 359, no. 6371, pp. 61–65, 2018.
- [7] N. Kellaris, V. Gopaluni Venkata, G. M. Smith, S. K. Mitchell, and C. Keplinger, "Peano-hasel actuators: Muscle-mimetic, electrohydraulic transducers that linearly contract on activation," *Science Robotics*, vol. 3, no. 14, p. eaar3276, 2018.
- [8] K. Ly, N. Kellaris, D. McMorris, B. K. Johnson, E. Acome, V. Sundaram, M. Naris, J. S. Humbert, M. E. Rentschler, C. Keplinger *et al.*, "Miniaturized circuitry for capacitive self-sensing and closed-loop control of soft electrostatic transducers," *Soft Robotics*, vol. 8, no. 6, pp. 673–686, 2021.
- [9] Z. Yoder, N. Kellaris, C. Chase-Markopoulou, D. Ricken, S. K. Mitchell, M. B. Emmett, R. F. f. Weir, J. Segil, and C. Keplinger, "Design of a high-speed prosthetic finger driven by peano-hasel actuators," *Frontiers in Robotics and AI*, vol. 7, p. 586216, 2020.
- [10] Z. Yoder, D. Macari, G. Kleinwaks, I. Schmidt, E. Acome, and C. Keplinger, "A soft, fast and versatile electrohydraulic gripper with capacitive object size detection," *Advanced Functional Materials*, vol. 33, no. 3, p. 2209080, 2023.
- [11] N. Kellaris, V. G. Venkata, P. Rothemund, and C. Keplinger, "An analytical model for the design of peano-hasel actuators with drastically improved performance," *Extreme Mechanics Letters*, vol. 29, p. 100449, 2019.
- [12] C. L. Collins, "Kinematics of robot fingers with circular rolling contact joints," *Journal of Robotic Systems*, vol. 20, no. 6, pp. 285–296, 2003.
- [13] Y. Toshimitsu, B. Forrai, B. G. Cangan, U. Steger, M. Knecht, S. Weirich, and R. K. Katzschmann, "Getting the ball rolling: Learning a dexterous policy for a biomimetic tendon-driven hand with rolling contact joints," in *2023 IEEE-RAS 22nd International Conference on Humanoid Robots (Humanoids)*. IEEE, 2023, pp. 1–7.
- [14] M. R. Cutkosky *et al.*, "On grasp choice, grasp models, and the design of hands for manufacturing tasks," *IEEE Transactions on robotics and automation*, vol. 5, no. 3, pp. 269–279, 1989.
- [15] T. Feix, J. Romero, H.-B. Schmiebmayer, A. M. Dollar, and D. Kragic, "The grasp taxonomy of human grasp types," *IEEE Transactions on human-machine systems*, vol. 46, no. 1, pp. 66–77, 2015.